NATIONAL ADVISORY COMMITTEE FOR AERONAUTICS

WARTIME REPORT

ORIGINALLY ISSUED

July 1946 as
Memorandum Report E6F03

EFFICIENCY OF A RADIAL-FLOW EXHAUST-GAS TURBOSUPERCHARGER

TURBINE WITH A 12.75-INCH TIP DIAMETER

By Earl E. Coulter, Robert G. Larkin, and David S. Gabriel

Aircraft Engine Research Laboratory
Cleveland, Ohio

NACA

WASHINGTON

NACA MR No. E6F03

NACA AIRCRAFT ENGINE RESEARCH LABORATORY

MEMORANDUM REPORT

for the

Bureau of Aeronautics, Navy Department

EFFICIENCY OF A RADIAL-FLOW EXHAUST-GAS TURBOSUPERCHARGER

TURBINE WITH A 12.75-INCH TIP DIAMETER

By Earl E. Coulter, Robert G. Larkin
and David S. Gabriel

SUMMARY

An investigation has been made of the effect on the performance of a radial-flow exhaust-gas turbosupercharger turbine with a 12.75-inch tip diameter of various inlet pressures, inlet temperatures, wheel speeds, pressure ratios, and cooling-air flows. For a given blade-to-jet speed ratio, variation in pressure ratio from 1.5 to 4.0 and inlet temperature from 800° to 1200° R had only a small effect on turbine efficiency. For blade-to-jet speed ratios of 0.5 and 0.6, the efficiency increased 4.5 points as inlet pressure increased from 20 to 50 inches of mercury absolute. Cooling-air flow had no measurable effect on turbine efficiency within the accuracy of the tests in the test range: namely, ratios of cooling-air flow to turbine gas flow from 0 to 14 percent, turbine pressure ratio of 2.0, turbine inlet total pressures from 15 to 40 inches of mercury absolute, and inlet temperatures from 800° to 2000° R.

INTRODUCTION

The radial-flow exhaust-gas turbine investigated has many features that are radically different from those of the conventional axial-flow turbine. The radial-flow turbine wheel runs with considerable reaction and incorporates drilled cooling-air passages through the disk. Performance tests of the conventional axial-flow turbine have been reported in references 1 and 2, but very little data have been published on the radial-flow-type turbine (reference 3) and no data are available that show the effect of cooling-air flow on turbine efficiency.

An investigation was therefore made at the NACA Cleveland laboratory during July and August 1945 at the request of the Bureau of Aeronautics, Navy Department, to determine the basic efficiency and also to investigate the effect of cooling-air flow on turbine performance. Curves of efficiency and air flow are presented that cover a range of turbine speeds from 3000 to 17,000 rpm, inlet pressures from 15 to 50 inches of mercury absolute, inlet temperatures from 800° to 2000° R, pressure ratios from 1.5 to 4.0, and cooling-air flows from 0 to 10 percent of the turbine gas flow.

TURBINE ASSEMBLY

A photograph of the setup for the investigation of the radial-flow exhaust-gas turbine is shown in figure 1. The nozzle box, the turbine wheel with cooling-air passages and shaft, the wheel-case center cover, and the rear-bearing support (turbine end of shaft) are shown in figure 2. The nozzle box is a double tangential-inlet radial-flow type. The turbine wheel has a comparatively small number of blades (17) and runs with considerable reaction; the driving fluid enters the turbine wheel radially and is discharged axially.

The compressor impellers and diffusers and the oil pump were removed. The waste gate was replaced by a stainless-steel seal to eliminate leakage. The oil passages in the front-bearing housings (compressor end of shaft) were reworked to permit lubrication of the bearings from external oil pumps. An extension shaft was inserted into and fastened to the compressor end of the hollow turbine shaft with dowel pins. The power was transmitted through a flexible coupling to a high-speed eddy-current dynamometer. Distortion of the wheel-case center cover and consequent rubbing on the turbine wheel at simulated altitude conditions were prevented by installing a chamber between the nozzle box and rear-bearing support and venting it to the turbine discharge duct. Figure 3 shows these modifications.

The clearance between the air seal (fig. 3) and the back of the turbine wheel was set at 0.005 inch cold and the clearance between the trailing edge of the turbine-blade tips and the turbine casing was 0.044 to 0.051 inch cold. The distance from the upstream end of the inner cylinder of the annular exhaust chamber to the turbine wheel was seven-eighths inch.

The wheel was designed to be cooled by air bled from the first-stage compressor to increase the life of the turbine wheel at elevated temperatures and to permit safe operation at inlet-gas temperatures up to 1700° R. Because the compressors were removed, cooling air had to be provided from an external source. The

compressor inlet and one outlet were blanked off and cooling air
from the laboratory air supply was introduced through the other
compressor outlet. Cooling-air flow was measured by a thin-plate
orifice. Fifty-one cooling-air passages are located in the turbine
wheel in planes slightly less than 90° from the turbine axis. (See
detail A of fig. 3.) These passages terminate in groups of three
into 17 other drilled passages, each one under the root of a blade
and roughly parallel to the root. The cooling air enters the wheel
near the shaft and discharges on the downstream side of the turbine
wheel near the axis. The air-flow path is indicated by arrows in
figure 3. The cooling-air passage outlets are shown in figure 2(b).
The turbine was driven by hot gas at various temperatures and
pressures from a hot-gas producer similar to the one described in
reference 1.

A plenum chamber in the form of an inverted U constructed from
18-inch-diameter ducts and covered with 3 inches of insulation was
attached to the nozzle box to insure an equal gas flow through both
nozzle-box inlets. This arrangement is shown in figure 1. The hot
gas entered at the center of the top of the chamber and flowed down
both legs. The nozzle-box inlet ducts extended into the legs of
the plenum chamber and the upstream ends were bellmouthed to induce
a smooth gas flow.

INSTRUMENTATION

A thin-plate orifice was used to measure air flow to the gas
producer. Fuel flow was measured with a calibrated rotameter.

Inlet-gas temperature was measured by four quadruple-shielded
chromel-alumel thermocouples, two placed in each inlet to the
nozzle box. The average of these four thermocouple readings was
assumed to be the total temperature at the nozzle-box inlets. The
maximum difference in thermocouple readings was ±5° F. Inlet static
pressure was taken as the average of the readings of eight pressure
taps, four located in the same cross section in each of the two
nozzle-box inlet ducts as indicated in figure 3. These pressure
readings had a maximum variation of ±0.1 inch of mercury. The total
inlet pressure was computed from the measured static pressure and
the total temperature by use of the continuity equation.

An annular chamber having the same cross-sectional area as
the annular area swept by the discharge edges of the turbine blades
plus the annular area that corresponds to the clearance between the
trailing edge of the blade tips and the turbine casing was provided
at the turbine discharge. Three banks of static pressure taps,
16 taps in each bank, were installed 120° apart in the annular

chamber. Six taps of each bank were installed in the outer cylinder of the annular chamber and 10 taps in the inner cylinder. These taps were spaced 0.75 inch and the six taps on the downstream end of the inner cylinder of the chamber were directly opposite the six taps in the outer cylinder of the annular chamber. The annular chamber and one bank of pressure taps are shown in figure 3. The turbine static discharge pressure was taken as the average of the readings of the six pressure taps lying in the plane passing through taps 1 and 11 (figure 3) and perpendicular to the axis of the turbine.

Dynamometer torque measurements were made with an NACA balanced-diaphragm torque indicator to the nearest 0.204 foot-pound. Turbine speed was measured to the nearest 10 rpm by two chronometric tachometers, each driven by its own tachometer generator turning at one-tenth turbine speed. The method recommended by the A.S.M.E. of estimating the accuracy of measurement of air flow gives a probable error of ±1.2 percent.

SYMBOLS

The following symbols are used in the report:

A_n actual turbine nozzle outlet area (sq ft)

g acceleration due to gravity, 32.2 (ft)/(sec)^2, or dimensional constant, 32.2 (lb)/(slug)

M_m theoretical maximum mass flow of gas that can be passed through convergent nozzle of 21.5-square-inch throat area, (slugs)/(sec)

M_t mass flow of air plus fuel, (slugs)/(sec)

N turbine speed, (rpm)

p_d static pressure of turbine discharge, (in. Hg absolute)

p_i total pressure at nozzle-box inlet, (in. Hg absolute)

R_b gas constant for combustion products, (ft-lb)/(lb-°R)

T_i total temperature at nozzle-box inlet, (°R)

u blade tip speed, (fps)

v theoretical jet speed, (fps)

W_c weight flow of cooling air, (lb)/(sec)

W_t weight flow of air plus fuel, (lb)/(sec)

γ ratio of specific heats

η turbine efficiency defined as ratio of shaft power to theoretical power computed from total temperature and pressure at turbine inlet and static pressure at turbine discharge

η' turbine efficiency defined as ratio of shaft power to difference between theoretical power (as defined for η) and kinetic power where kinetic power is calculated from average axial component of velocity at turbine discharge

δ ratio of turbine inlet pressure to NACA standard sea-level pressure, $p_1/29.92$

θ ratio of turbine inlet temperature to NACA standard sea-level temperature, $T_1/519$

TEST CONDITIONS

The fundamental efficiency of the turbine was determined by tests without cooling air. These tests were limited to an inlet temperature of 1200° R. The approximate test conditions were as follows:

Total inlet pressure, p_1 (in. Hg abs.)	Total inlet temperature, T_1 (°R)	Pressure ratio p_1/p_d
15	1200	1.5, 2.0
20	1000	1.5
30	800 1000 1200	1.5, 2.0, 3.0, 4.0
30	900 1100	2.0, 4.0
40 50	1000 1000	1.5, 3.0, 4.0

At each condition, data were taken over a range of speeds up to the maximum obtainable, but the speed was limited to 17,000 rpm by the manufacturer.

   The gas temperatures for these tests were relatively low and
resulted in very low fuel-air ratios; consequently, the gas
properties differed little from those of air at these temperatures.
The turbine efficiency η based on the total inlet pressure and
temperature and the static discharge pressure was calculated by
using a table of the thermodynamic properties of air from
reference 4 and the equations of reference 5. The efficiency η'
based on the difference between the total available energy calcu-
lated from the static discharge pressure and total inlet temperature
and pressure and the kinetic energy of the average axial component
of discharge velocity was calculated by the method of reference 1.
Values of R_b and γ, taken from reference 6, were used to calcu-
late the average axial component of the discharge velocity.

   Additional tests were made at a constant pressure ratio of 2.0
to investigate the effect of cooling air on turbine efficiency. The
following table shows the approximate conditions for each test:

Total inlet pressure, p_1 (in. Hg. abs.)	Total inlet temperature, T_1 ($^\circ$R)	Cooling-air flow W_c (lb/sec)
15	1200	0, 0.095, 0.195
30	800	0, 0.095, 0.196, 0.330
	1200	0, 0.095, 0.196, 0.330
	1600	0.195, 0.330, 0.410
	2000	0.330, 0.410
40	1200	0.095, 0.196, 0.330

At each test condition the speed was varied up to the maximum
obtainable but limited to 17,000 rpm. The cooling-air flows
selected were chosen to insure safe operation of the turbine and
were not necessarily the minimum flows required for cooling.

   At the conclusion of this test program, a sudden increase in
air flow of about 2 percent was noted. Inspection of the nozzle
box revealed several radial cracks about one-half inch long and
one-sixteenth inch wide in the casting that forms the waste-gate
nozzles. The stress introduced by the waste-gate seal clamped over
the casting may possibly have been the cause of these cracks.

                              RESULTS

   The results of the tests without cooling air are shown
in table I.

Turbine efficiency η is plotted against blade-to-jet speed ratio in figures 4 and 5. Figure 4 demonstrates the effect of pressure ratio for three inlet total gas temperatures and figure 5 shows the effect of inlet temperature and pressure on turbine efficiency. The peak efficiency occurs at a blade-to-jet speed ratio of about 0.66.

Figure 6(a) shows that for blade-to-jet speed ratios lower than 0.6 the turbine efficiency increases with increase in pressure ratio up to 3.0 and then decreases. For a blade-to-jet speed ratio of 0.4 the increase is about 2 points for an increase in pressure ratio from 1.5 to 3.0. For a blade-to-jet speed ratio of 0.6, however, the efficiency decreases about 2 points when the pressure ratio increases from 1.5 to 3.0. Figure 6(b) shows the effect of variation in inlet temperature on turbine efficiency. The turbine efficiency varies only slightly with inlet temperature. Over the range of inlet temperatures from 800° to 1200° R the maximum difference in efficiency was 1.5 points. The efficiency increases with inlet pressure as shown in figure 6(c). The greatest increase of efficiency occurs at blade-to-jet speed ratios of 0.5 and 0.6 and is about 4.5 points over a range of inlet pressures from 20 to 50 inches of mercury absolute.

In figure 7 the turbine efficiency is plotted against the Reynolds number factor $p_i/T_i^{1.1}$ derived in reference 1. The curves are shown for constant blade-to-jet speed ratios from 0.2 to 0.6 and pressure ratios from 1.5 to 4.0. The inlet-pressure range shown is from 15 to 50 inches of mercury absolute and the inlet-temperature range is from 800° to 1200° R. The derivation of the Reynolds number factor in reference 1 neglects mechanical losses, bearing friction, and windage, which is a logical assumption when small turbines having antifriction bearings are considered. Friction losses are, however, considerably higher for journal-type bearings and would have proportionally greater influence on the results. No correction has been made in the data reported here for bearing friction. Although figure 7 shows a good correlation of the data, it cannot be offered as evidence of the effect of Reynolds number on turbine efficiency because of the small variation of the efficiency with the Reynolds number factor and the unknown effect of bearing friction.

The turbine mass flow may be correlated by plotting the gas-flow factor $\dfrac{M_t}{p_1}\sqrt{gR_bT_1}$ (reference 1) against the speed factor $N/\sqrt{\theta}$ for any pressure ratio. For convenience of calculation, the gas-flow factor is reduced to the form $(M_t\sqrt{\theta})/\delta$ and plotted against the

speed factor for various pressure ratios in figure 8. All the data
over the range of inlet pressures and temperatures is correlated on
this plot within an accuracy of $1\frac{3}{4}$ percent. The variation of the
gas-flow factor $(M_t \sqrt{\theta})/\delta$ with pressure ratio is shown on cross
plot figure 9. The occurrence of reaction is indicated by the fact
that the gas-flow factor continues to increase as the pressure ratio
increases above 1.83.

The ratio of the turbine mass flow M_t to the critical mass
flow M_m at any given inlet pressure and temperature is plotted
against the speed factor $N/\sqrt{\theta}$ in figure 10. The critical mass
flow is defined as the theoretical maximum flow that could be
passed through a convergent nozzle having a discharge area equivalent
to the turbine nozzle discharge area (21.5 sq in.) and is calculated
from the following equation:

$$M_m = \frac{70.73 \, p_1 A_n}{\sqrt{g R_b T_1}} \left(\frac{2}{\gamma+1}\right)^{\frac{1}{\gamma-1}} \sqrt{\frac{2\gamma}{\gamma+1}}$$

Although γ and R vary with inlet temperature, their
variation with temperature over a range from $800°$ to $1200°$ R
resulted in a difference in M_m of less than one-half percent.
Consequently, for all practical purposes equation (1) reduces to

$$(M_m \sqrt{\theta})/\delta = 0.228 \ (\text{slug})/(\text{sec})$$

where

$$\gamma = 1.380$$

$$R_b = 53.25 \ (\text{ft-lb})/(\text{lb})(°R)$$

The plot of figure 10 correlates all the data over the entire range
of test conditions. Figure 11 is a cross plot of figure 10 and
shows that the ratio M_t/M_m approaches a value of 0.875 at a pressure
ratio of about 4.0.

Turbine efficiency η' is plotted against blade-to-jet speed
ratio for various inlet temperatures and pressure ratios in
figure 12 and data are shown for the same conditions as those of
figure 4. In this case the efficiency η' increases with pressure
ratio for each inlet temperature.

A plot of the efficiency ratio η'/η against the blade-to-jet speed ratio for various pressure ratios is shown in figure 13, which correlates all the data within an accuracy of 1 percent. The efficiency η' varies from 1.04 to 1.16 times the corresponding values of η. The greatest increase occurs at the combination of low blade-to-jet speed ratios and high pressure ratios.

The results of the tests using turbine-wheel cooling air are shown in figure 14, a typical curve of turbine efficiency plotted against blade-to-jet speed ratio for various cooling-air flows from 0 to approximately 0.33 pound per second. These data were taken with an inlet pressure of approximately 30 inches of mercury absolute and an inlet temperature of 800° R. It is evident from this plot that for the range investigated cooling-air flow has no measurable effect on turbine efficiency within the accuracy of the data.

The effect of cooling air on the turbine efficiency is shown in the following summary table:

Inlet total temperature, T_1 (°R)	Inlet total pressure, p_1 (in. Hg abs.)	Blade-to-jet speed ratio u/v	Cooling-air flow (percent turbine gas flow)	Turbine efficiency η
800	29.8	0.6	0 - 7	0.675
1200	29.8	.6	$0 - 8\frac{1}{4}$	.67
1600	29.8	.5	$5\frac{1}{2} - 12\frac{1}{4}$	.61
2000	29.8	.45	$10\frac{1}{2} - 13\frac{3}{4}$	.58
1200	39.9	.55	$0 - 6\frac{1}{4}$	.65
1200	29.8	.55	$0 - 8\frac{1}{4}$	.65
1200	14.8	.55	$0 - 10$	.61

No variation in efficiency with cooling-air flow is noted in this table. Figure 14 and this table show only the effect of the cooling-air flow on the performance of the turbine proper. A complete evaluation of the cooling-power loss must include the pumping horsepower required to force the cooling air through the cooling passages. Table II shows a summary of the test data using cooling air and

includes the cooling-air flow, pressure drop from the compressor housing to the turbine discharge pressure, and cooling-air inlet temperature measured just before entrance to the turbine wheel. From these data the pumping horsepower can be computed. A correlation of this cooling data was not attempted because the temperature variation of the cooling air as it passed through the cooling passages was unknown.

SUMMARY OF RESULTS

From efficiency tests of a radial-flow exhaust-gas turbo-supercharger turbine with a 12.75-inch tip diameter over a range of pressure ratios, inlet temperatures, inlet pressures, and cooling-air flows, the following results were obtained:

1. The variation of efficiency with pressure ratio over the range from 1.5 to 4.0 was small (2 points or less) for any given blade-to-jet speed ratio.

2. The turbine efficiency varied only slightly with inlet temperature. Over the inlet-temperature range from 800° to 1200° R, the maximum difference in efficiency was 1.5 points.

3. The efficiency increased about 4.5 points at blade-to-jet speed ratios of 0.5 and 0.6 as inlet pressure increased from 20 to 50 inches of mercury absolute.

4. The mass flow through the turbine increased with pressure ratio and approached a limiting value at a pressure ratio of about 4.0. At a pressure ratio of 4.0, the ratio of the turbine mass flow to the theoretical maximum mass flow was 0.875.

5. Tests made with turbine inlet-gas pressures from 15 to 40 inches of mercury absolute, inlet-gas temperatures from 800° to 2000° R, a pressure ratio of 2.0, and cooling-air flows up to 14 percent of the turbine gas flow show that cooling-air flow had no measurable effect on turbine efficiency.

Aircraft Engine Research Laboratory,
    National Advisory Committee for Aeronautics,
        Cleveland, Ohio.

REFERENCES

1. Gabriel, David S., Carman, L. Robert, and Trautwein, Elmer E.:
   The Effect of Inlet Pressure and Temperature on the Efficiency
   of a Single-Stage Impulse Turbine Having an 11.0-Inch Pitch-
   Line Diameter Wheel. NACA ACR No. E5E19, 1945.

2. Chanes, Ernest R., and Carman, L. Robert: The Effect of Inlet
   Temperature and Pressure on the Efficiency of a Single-Stage
   Impulse Turbine Having a 13.2-Inch Pitch-Line Diameter Wheel.
   NACA ARR No. E5H10, 1945.

3. Maurer, R. J.: Performance Test of Turbo Engineering Corporation
   Turbo Supercharger. Ser. No. AEL-770, Aero. Eng. Lab.,
   Naval Air Material Center, Naval Air Exp. Sta. (Philadelphia),
   Bur. Aero., Navy Dept., July 29, 1944.

4. Keenan, Joseph H., and Kaye, Joseph: Thermodynamic Properties
   of Air. John Wiley & Sons, Inc. 1945, pp. 3-20.

5. Gabriel, David S., and Carman, L. Robert: Efficiency Tests of a
   Single-Stage Impulse Turbine Having an 11.0-Inch Pitch-Line
   Diameter Wheel with Air as the Driving Fluid. NACA ACR E5C30,
   1945.

6. Pinkel, Benjamin, and Turner, L. Richard: Thermodynamic Data
   for the Computation of the Performance of Exhaust-Gas Turbines.
   NACA ARR No. 4B25, 1944.

TABLE I – SUMMARY OF TEST DATA WITHOUT COOLING AIR

Left panel:

Pressure ratio p_1/p_4	Total inlet pressure (in. Hg abs.) p_1	Total-inlet temperature T_1 (°R)	Turbine speed N (rpm)	Blade-to-jet speed ratio u/v	Shaft power (hp)	Gas flow W_t (lb/sec)	Turbine efficiency η	η'
1.48	14.8	1200	3,000	0.135	14.7	1.63	0.210	0.219
1.49	14.8		5,980	.266	27.2	1.65	.273	.389
1.50	14.8		7,440	.329	33.0	1.66	.445	.465
1.50	14.8		9,030	.400	37.6	1.66	.509	.531
1.49	14.8		10,490	.466	62.8	1.66	.556	.580
1.50	14.8		11,900	.528	44.0	1.66	.599	.624
1.50	14.8		8,010	.354	34.0	1.65	.660	.680
1.99	14.8	1200	3,000	0.104	22.5	1.87	0.165	0.175
1.99	14.9		6,010	.208	41.7	1.90	.299	.318
2.00	14.9		7,510	.258	51.2	1.91	.363	.385
2.00	14.9		9,000	.310	59.3	1.92	.420	.445
2.00	14.9		10,490	.362	66.2	1.92	.469	.497
2.00	14.9		12,000	.414	75.7	1.92	.536	.567
2.00	14.8		13,480	.464	80.3	1.91	.571	.603
2.02	14.9		15,040	.516	84.3	1.91	.594	.627
2.01	14.9		16,350	.562	87.1	1.91	.616	.650
1.50	19.8	1000	3,000	0.145	20.2	2.41	0.225	0.235
1.50	19.9		6,010	.291	38.5	2.42	.427	.448
1.50	19.9		7,510	.363	44.0	2.41	.488	.508
1.50	19.8		9,010	.437	40.7	2.43	.550	.574
1.50	19.8		10,510	.510	52.7	2.39	.594	.618
1.49	19.8		11,970	.584	54.5	2.37	.627	.652
1.50	19.7		13,500	.655	55.7	2.35	.640	.665
1.50	19.8		11,550	.562	53.4	2.38	.609	.633
1.49	29.7	800	2,990	0.164	29.5	4.02	0.252	0.263
1.50	29.7		5,990	.326	55.4	4.13	.454	.474
1.50	29.7		7,550	.411	65.5	4.14	.536	.560
1.50	29.7		9,010	.489	73.5	4.11	.604	.630
1.49	29.6		10,500	.575	78.7	4.06	.657	.684
1.48	29.6		11,960	.656	78.9	3.99	.683	.710
1.49	29.7		13,470	.735	78.4	3.99	.670	.697
1.49	29.8		14,970	.819	72.5	3.96	.627	.652
1.97	29.7	800	2,990	0.128	46.4	4.69	0.206	0.219
1.99	29.7		6,020	.255	88.7	4.71	.388	.411
2.00	29.7		7,510	.318	104.0	4.75	.448	.475
2.01	29.7		9,010	.380	120.9	4.72	.522	.552
1.99	29.7		10,490	.446	132.2	4.69	.583	.615
1.99	29.7		11,970	.506	143.5	4.75	.624	.658
1.99	29.7		13,490	.571	148.6	4.69	.652	.686
1.98	29.6		14,990	.638	151.2	4.63	.679	.714
1.98	29.7		17,000	.723	150.4	4.64	.671	.705
2.97	29.6	800	3,000	0.104	62.4	5.00	0.172	0.190
2.98	29.5		6,020	.208	117.7	5.04	.320	.352
3.01	29.6		7,520	.259	143.8	5.08	.386	.424
3.00	29.6		9,000	.311	167.2	5.09	.449	.491
2.99	29.7		10,500	.363	187.5	5.12	.502	.548
3.02	29.8		12,000	.413	208.5	5.11	.555	.604
3.01	29.6		13,500	.465	224.7	5.10	.600	.651
3.00	29.8		15,020	.518	237.1	5.09	.635	.688
2.96	29.6		16,990	.590	241.2	5.08	.656	.709
4.04	29.7	800	6,000	0.187	133.3	5.14	0.290	0.334
3.95	29.6		7,500	.236	161.5	5.16	.354	.405
4.00	29.8		9,000	.282	191.1	5.18	.415	.472
3.94	29.6		10,490	.330	214.6	5.20	.468	.530
3.93	29.7		12,000	.378	240.3	5.22	.523	.588
3.95	29.7		13,500	.425	262.3	5.20	.571	.640
3.93	29.7		15,040	.474	278.9	5.16	.614	.683
3.93	29.7		17,040	.537	293.4	5.21	.640	.713
1.49	29.8	1000	3,050	0.149	31.1	3.63	0.234	0.245
1.50	29.8		6,030	.293	57.5	3.69	.421	.440
1.49	29.7		7,520	.366	69.1	3.69	.506	.529
1.50	29.8		9,000	.436	77.8	3.71	.563	.588
1.50	29.9		10,490	.508	85.8	3.69	.626	.652
1.50	29.7		11,980	.587	86.4	3.61	.656	.683
1.49	29.8		13,490	.658	87.3	3.58	.665	.692
1.50	29.9		14,960	.723	88.7	3.59	.660	.687
1.95	29.7	1000	3,010	0.116	46.3	4.17	0.189	0.200
1.97	29.7		5,990	.229	87.5	4.20	.349	.370
1.98	29.7		7,510	.286	106.8	4.22	.421	.446
1.97	29.6		9,000	.343	122.8	4.24	.481	.510
1.97	29.7		10,480	.400	138.1	4.27	.539	.570
1.99	29.7		11,990	.455	152.4	4.24	.591	.625
1.99	29.7		13,500	.511	162.7	4.25	.630	.665
1.98	29.8		14,970	.569	166.5	4.22	.653	.688
1.98	29.8		16,990	.646	169.2	4.16	.673	.708
2.94	29.7	1000	2,980	0.093	61.8	4.49	0.152	0.169
2.95	29.7		6,010	.187	121.1	4.53	.295	.325
2.94	29.7		7,510	.234	147.1	4.55	.358	.395
2.96	29.8		9,010	.279	171.1	4.55	.414	.453
2.95	29.6		10,500	.326	192.5	4.55	.468	.511
2.96	29.8		11,990	.371	213.3	4.55	.515	.561
2.97	29.7		13,540	.418	234.5	4.55	.564	.613
2.98	29.6		15,010	.468	249.5	4.55	.601	.652
2.96	29.8		16,980	.527	262.5	4.55	.636	.688
2.95	29.9		12,010	.372	213.6	4.56	.516	.562
2.93	29.8		7,600	.237	147.0	4.53	.360	.395
4.21	29.8	1000	7,540	0.208	164.8	4.63	0.310	0.360
4.05	29.8		9,010	.251	193.1	4.59	.373	.426
4.02	29.9		10,500	.293	219.3	4.60	.426	.484
4.02	29.8		12,000	.335	246.9	4.62	.478	.541
3.98	29.7		13,490	.378	270.2	4.61	.527	.593
3.99	29.6		15,010	.420	291.8	4.60	.569	.638
3.96	29.8		17,040	.478	315.3	4.60	.618	.688
1.49	29.7	1200	3,000	0.134	30.9	3.32	0.214	0.223
1.49	29.7		6,000	.267	57.4	3.35	.388	.405
1.50	29.9		7,500	.332	69.7	3.37	.465	.486
1.50	29.9		8,990	.399	79.0	3.37	.529	.552
1.50	29.8		10,470	.463	86.8	3.35	.581	.606
1.50	29.8		11,960	.529	94.0	3.33	.631	.658
1.49	29.7		13,430	.598	93.0	3.29	.641	.667
1.50	29.8		14,960	.664	93.1	3.27	.642	.667
1.99	29.9	1200	3,050	0.106	48.6	3.82	0.175	0.186
1.99	29.9		6,010	.208	90.9	3.87	.321	.341
2.00	29.9		7,490	.258	110.4	3.88	.386	.410
2.01	29.9		9,030	.311	126.2	3.88	.447	.474
2.01	29.9		10,490	.363	143.2	3.89	.498	.527
1.99	29.9		11,990	.414	157.2	3.90	.551	.583
2.00	29.9		13,470	.464	171.9	3.91	.597	.631
2.01	29.8		14,910	.512	181.0	3.89	.628	.663
2.01	29.8		17,010	.584	186.6	3.86	.652	.687

Right panel:

Pressure ratio p_1/p_4	Total inlet pressure (in. Hg abs.) p_1	Total-inlet temperature T_1 (°R)	Turbine speed N (rpm)	Blade-to-jet speed ratio u/v	Shaft power (hp)	Gas flow W_t (lb/sec)	Turbine efficiency η	η'
2.99	29.8	1200	3,010	0.085	84.9	4.11	0.144	0.159
2.99	30.0		6,000	.169	124.2	4.13	.273	.301
2.97	29.3		7,480	.211	150.1	4.14	.331	.364
2.99	29.8		9,010	.254	176.7	4.16	.385	.423
3.00	29.9		10,510	.295	199.5	4.17	.433	.475
3.01	29.9		12,000	.337	220.3	4.17	.479	.523
3.01	29.9		13,370	.376	241.3	4.17	.523	.570
3.01	29.8		14,950	.420	263.4	4.17	.570	.621
			16,970	.476	281.3	4.15	.613	.665
4.21	29.8	1200	7,520	0.189	168.5	4.20	0.290	0.337
4.26	29.8		9,000	.225	198.5	4.25	.338	.392
4.29	30.0		10,460	.261	223.8	4.25	.377	.436
4.29	29.9		11,970	.299	250.9	4.24	.424	.488
4.00	29.9		13,460	.343	276.9	4.23	.487	.551
3.99	29.8		15,040	.384	304.7	4.23	.538	.605
3.99	29.9		17,010	.434	332.7	4.24	.585	.656
1.97	29.8	900	2,990	0.120	45.8	4.37	0.194	0.206
1.99	29.6		6,020	.241	86.6	4.40	.360	.382
1.99	29.7		7,520	.300	106.5	4.43	.439	.465
1.99	29.6		9,000	.359	119.1	4.43	.491	.519
2.00	29.6		10,510	.419	137.0	4.47	.559	.591
1.99	29.7		11,990	.480	147.4	4.45	.608	.641
2.00	29.6		13,490	.538	155.4	4.42	.640	.675
2.00	29.8		14,950	.595	161.8	4.40	.668	.703
1.99	29.7		17,000	.676	160.9	4.39	.666	.700
			9,100	.364	123.6	4.48	.504	.534
3.99	29.7	900	7,530	0.222	164.0	4.86	0.337	0.386
4.03	29.7		9,000	.265	192.6	4.84	.396	.450
4.01	29.7		10,500	.310	218.5	4.87	.448	.507
3.96	29.6		12,020	.356	245.0	4.90	.502	.565
3.96	29.7		13,490	.400	266.5	4.88	.554	.620
3.97	29.8		15,000	.444	288.7	4.89	.591	.661
3.95			16,990	.503	302.6	4.89	.630	.702
1.98	29.9	1100	3,030	0.110	48.0	3.97	0.182	0.193
2.00	29.9		6,010	.217	90.5	4.04	.334	.354
2.00	29.9		7,530	.271	109.6	4.06	.401	.425
1.99	29.9		9,050	.327	126.7	4.08	.464	.491
2.00	29.8		10,500	.379	141.7	4.07	.518	.549
2.00	30.0		12,010	.433	156.5	4.08	.571	.603
2.00	29.8		13,500	.486	168.6	4.09	.612	.647
1.99	29.8		14,990	.540	176.1	4.06	.644	.680
1.99	29.9		16,980	.613	178.3	4.02	.663	.699
4.09	29.9	1100	7,550	0.200	168.0	4.44	0.305	0.352
3.94	29.7		9,000	.241	195.4	4.38	.367	.418
4.01	29.9		10,490	.279	222.4	4.41	.410	.467
3.99	29.8		12,020	.321	250.6	4.45	.459	.521
3.98	29.6		13,480	.360	275.2	4.40	.511	.576
3.98	29.6		15,000	.401	296.3	4.44	.545	.614
3.95	29.8		17,020	.455	324.3	4.44	.599	.670
1.48	39.4	1000	3,000	0.148	40.7	4.86	0.234	0.244
1.48	39.4		6,030	.296	71.8	4.88	.424	.443
1.49	39.7		7,540	.372	90.6	4.92	.498	.520
1.50	39.7		9,020	.459	103.1	4.93	.567	.592
1.50	39.7		10,480	.509	114.5	4.95	.625	.652
1.50	39.8		11,970	.579	122.5	4.90	.670	.697
1.50	39.7		13,470	.654	120.1	4.81	.675	.703
1.50	39.7		14,950	.730	131.6	4.76	.665	.691
1.48	39.7		17,000	.839	100.1	4.69	.596	.620
2.97	39.7	1000	3,020	0.094	85.6	5.94	0.158	0.175
2.97	39.6		6,020	.186	160.5	6.03	.292	.322
2.98	39.7		7,530	.253	197.0	6.01	.360	.394
3.00	39.7		9,040	.279	230.5	6.10	.412	.452
3.00	39.6		10,500	.324	260.0	6.07	.467	.510
2.99	39.5		12,000	.371	290.6	6.14	.518	.566
3.00	39.5		13,480	.416	318.6	6.10	.569	.619
2.98	39.5		15,...	.462	331.6	6.05	.597	.650
2.98	39.3		17,040	.527	356.6	6.00	.607	.704
4.11	39.7	1000	7,540	0.209	224.3	6.18	0.322	0.371
4.12	39.6		9,000	.250	261.4	6.18	.377	.428
4.13	40.0		10,480	.291	299.9	6.21	.426	.486
4.07	39.6		11,940	.332	334.2	6.22	.477	.541
4.03	40.0		13,490	.377	367.1	6.17	.531	.597
4.02	39.9		14,990	.419	399.8	6.20	.577	.647
4.06	39.9		16,990	.475	424.7	6.21	.614	.686
1.49	49.8	1000	2,990	0.146	53.0	6.06	0.238	0.249
1.50	49.7		6,030	.292	100.8	6.21	.435	.454
1.50	49.7		7,510	.364	119.1	6.18	.519	.542
1.50	49.6		8,970	.434	133.9	6.19	.582	.607
1.50	49.7		10,480	.507	146.7	6.18	.637	.664
1.50	49.8		12,020	.584	151.8	6.09	.671	.698
1.50	49.8		13,500	.655	154.8	6.08	.686	.714
1.50	49.8		14,980	.725	152.0	5.96	.684	.711
1.49	50.0		17,020	.831	140.3	5.96	.643	.669
2.94	49.6	1000	2,990	0.092	106.0	7.53	0.154	0.170
2.97	49.7		6,040	.187	205.5	7.53	.299	.308
2.96	49.7		7,520	.233	249.7	7.61	.361	.397
2.99	49.7		9,020	.279	286.9	7.59	.413	.452
2.99	49.4		10,470	.323	326.9	7.59	.469	.513
2.99	50.0		11,980	.370	363.5	7.63	.520	.567
3.02	50.0		13,490	.415	401.2	7.68	.566	.617
3.01	50.0		15,000	.462	425.5	7.59	.609	.660
2.99	49.9		16,980	.525	451.6	7.62	.648	.701
4.10	49.9	1000	7,520	0.209	277.8	7.70	0.319	0.368
4.04	49.9		9,000	.251	323.7	7.71	.375	.428
4.04			10,530	.294	371.7	7.81	.424	.484
4.01	50.0		12,010	.336	417.5	7.78	.481	.544
3.96	49.6		13,430	.377	451.7	7.78	.524	.590
3.97	49.8		14,980	.420	491.6	7.76	.569	.639
3.94			17,000	.478	527.5	7.76	.615	.687

TABLE II - SUMMARY OF TEST DATA WITH COOLING AIR

Pressure ratio p_1/p_4	Total inlet pressure p_1 (in. Hg abs.)	Total inlet temperature T_1 (°R)	Turbine speed N (rpm)	Blade-to-jet speed ratio u/v	Shaft power (hp)	Gas flow W_g (lb/sec)	Turbine efficiency η	Cooling-air flow W_c (lb/sec)	Cooling-air pressure drop (in. Hg)	Cooling-air inlet temperature (°R)

(Numeric data in this section is too small and densely printed to transcribe reliably.)

Pressure ratio p_1/p_4	Total inlet pressure p_1 (in. Hg abs.)	Total inlet temperature T_1 (°R)	Turbine speed N (rpm)	Blade-to-jet speed ratio u/v	Shaft power (hp)	Gas flow W_g (lb/sec)	Turbine efficiency η	Cooling-air flow W_c (lb/sec)	Cooling-air pressure drop (in. Hg)	Cooling-air inlet temperature (°R)

(Numeric data in this section is too small and densely printed to transcribe reliably.)
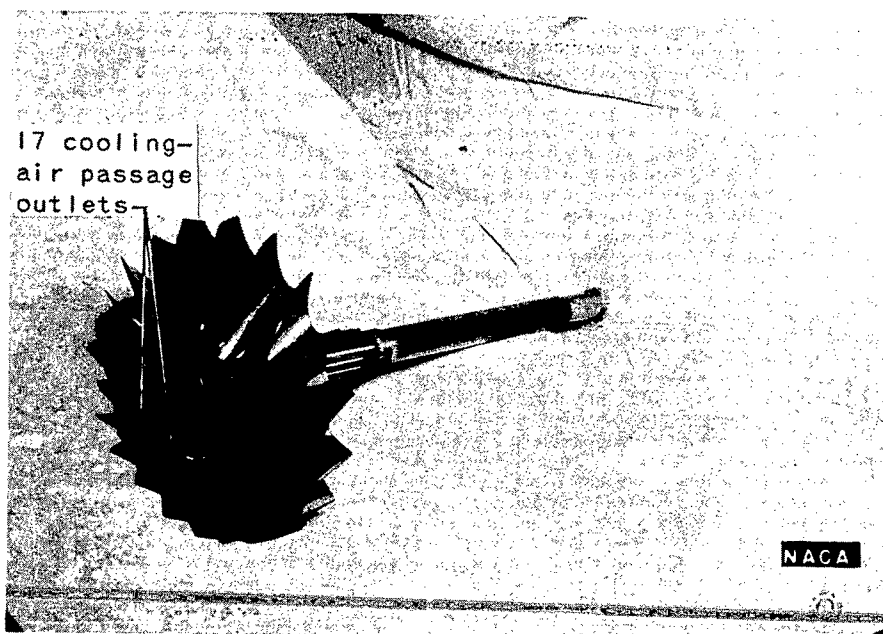
Figure I. — Test setup of radial—flow exhaust—gas turbosupercharger turbine.
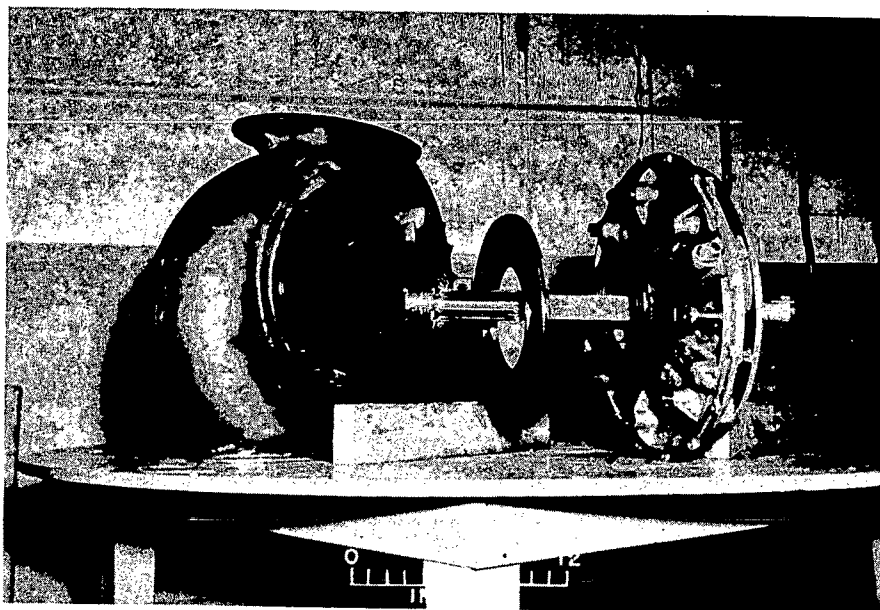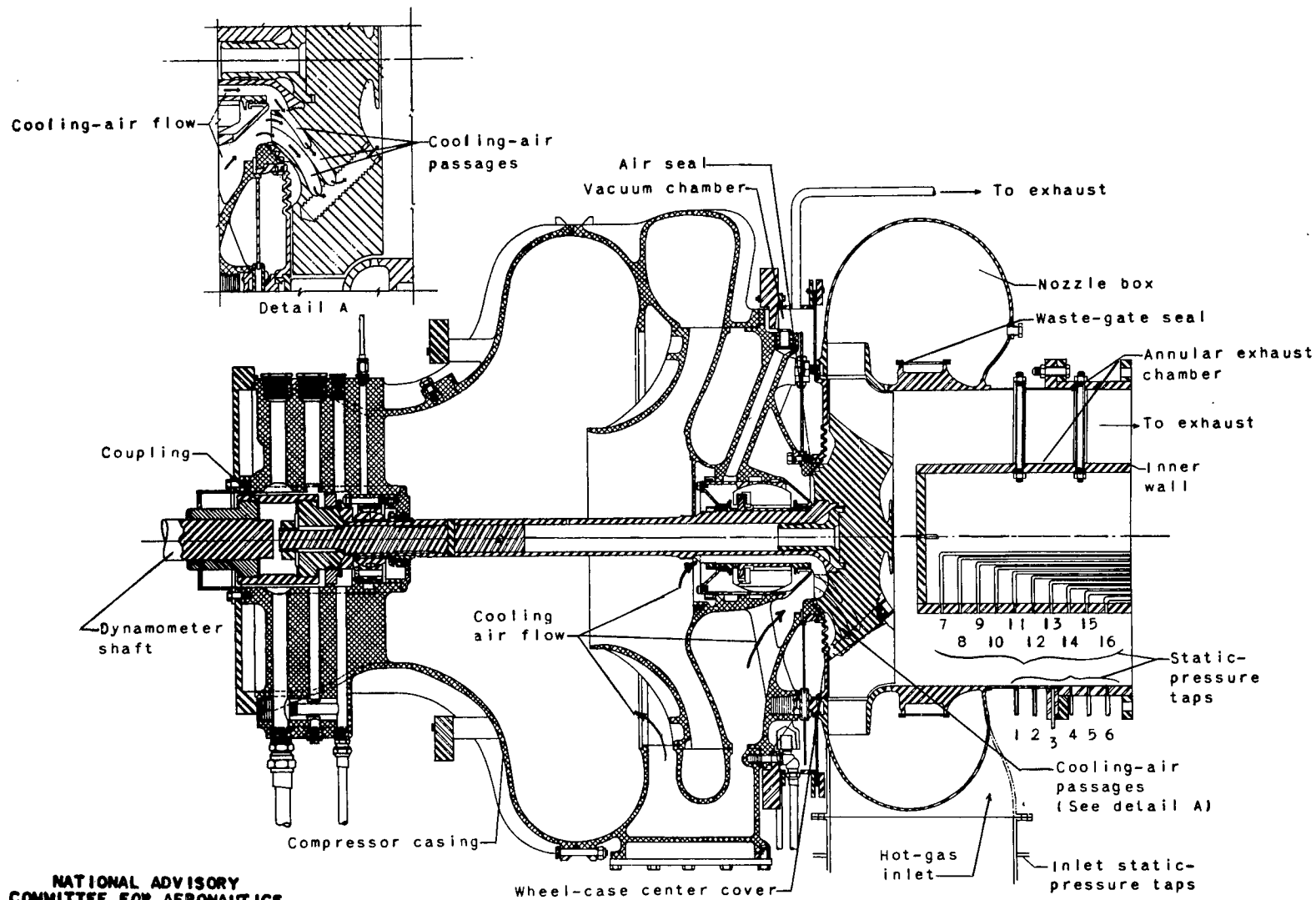
(a) Nozzle box, turbine wheel and shaft, wheel-case center
cover, and rear-bearing support.

(b) Turbine wheel showing cooling-air passage outlets.

Figure 2. - Components of radial-flow exhaust-gas turbosupercharger turbine.

Figure 3. – Schematic drawing of modified turbosupercharger assembly.
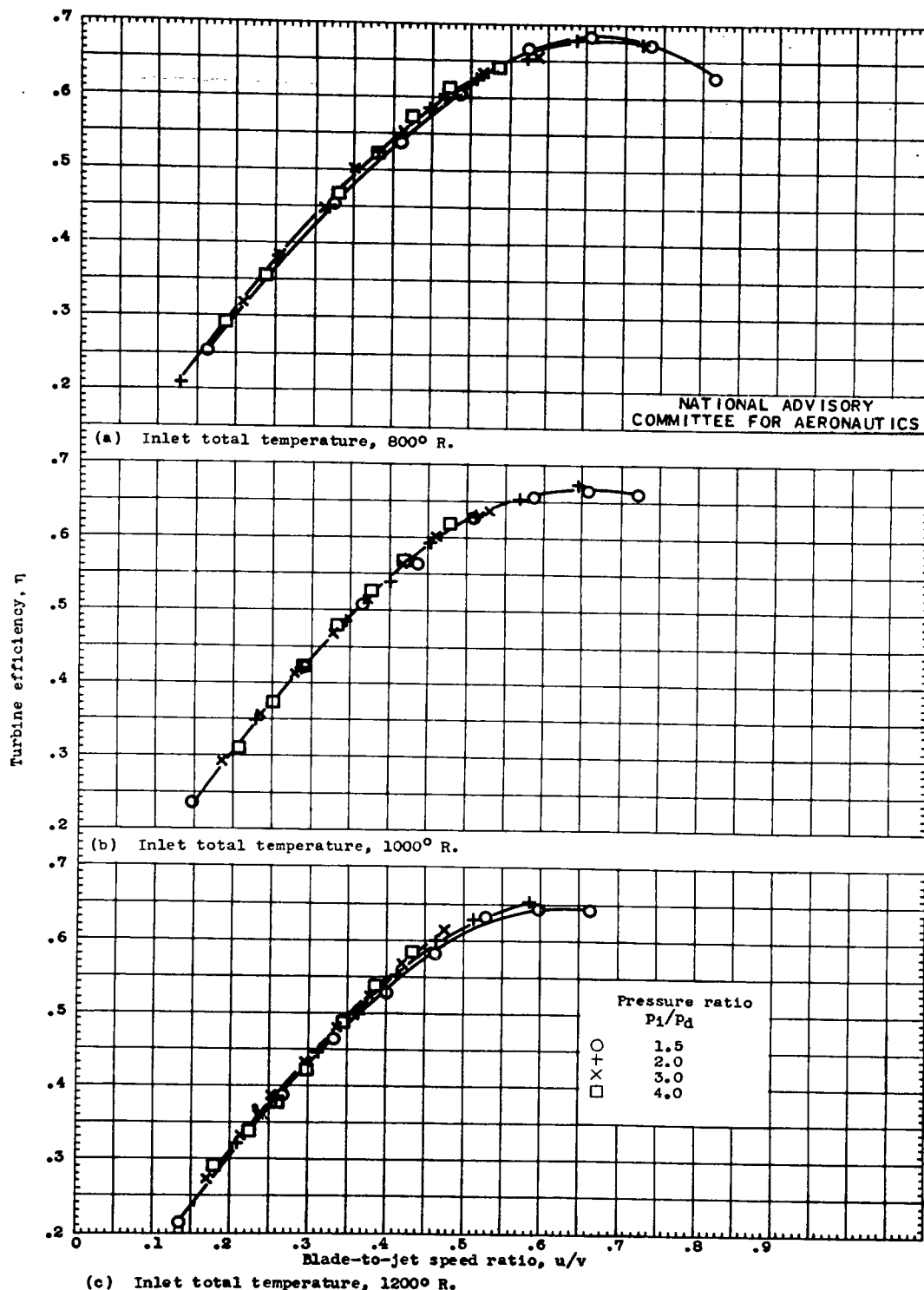
Figure 4. – Variation of turbine efficiency with blade-to-jet speed ratio for various inlet total temperatures and pressure ratios. Inlet total pressure, 29.8 inches of mercury absolute.
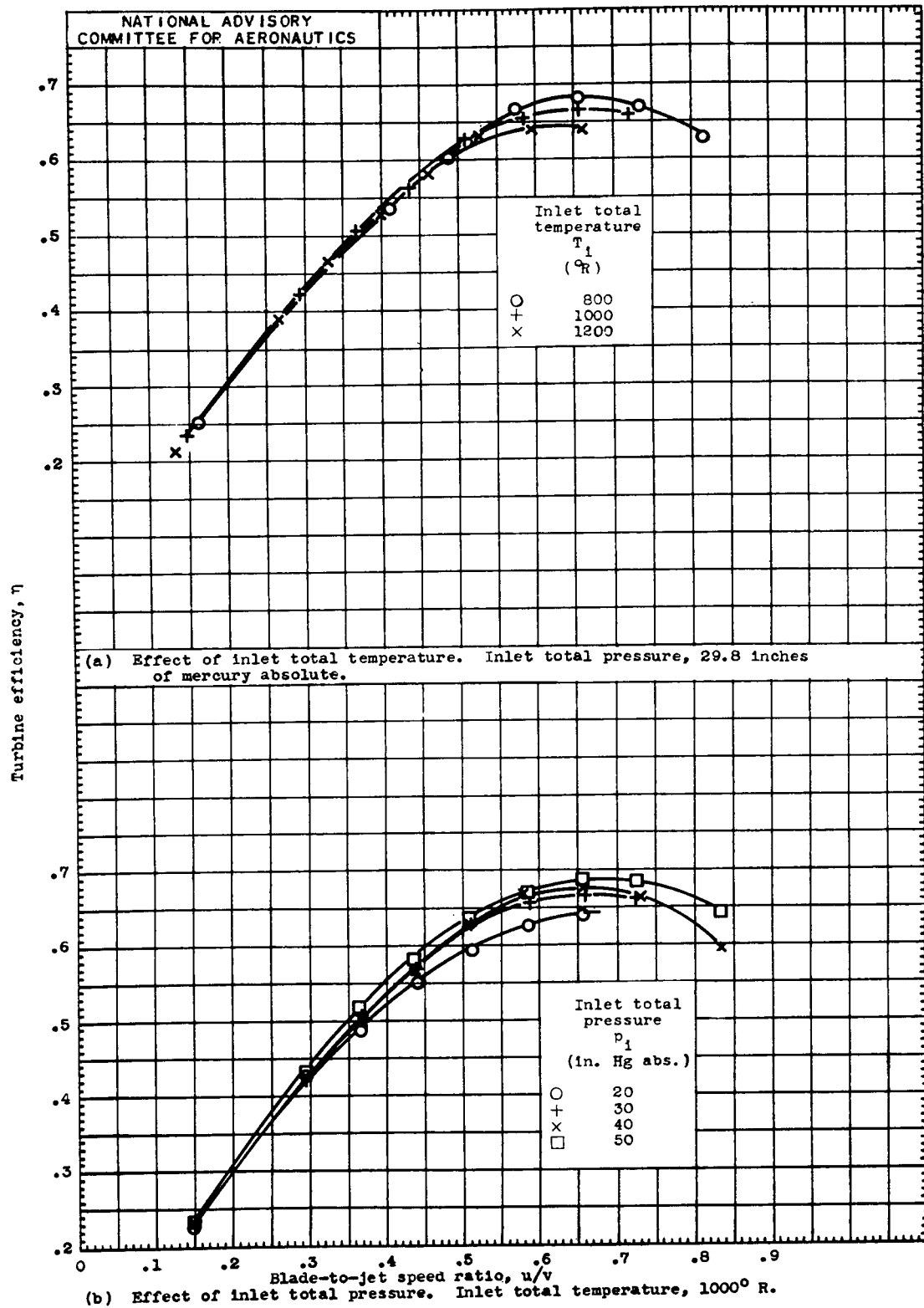
Figure 5. — Variation of turbine efficiency with blade-to-jet speed ratio for various inlet total temperatures and inlet total pressures. Pressure ratio, 1.5.
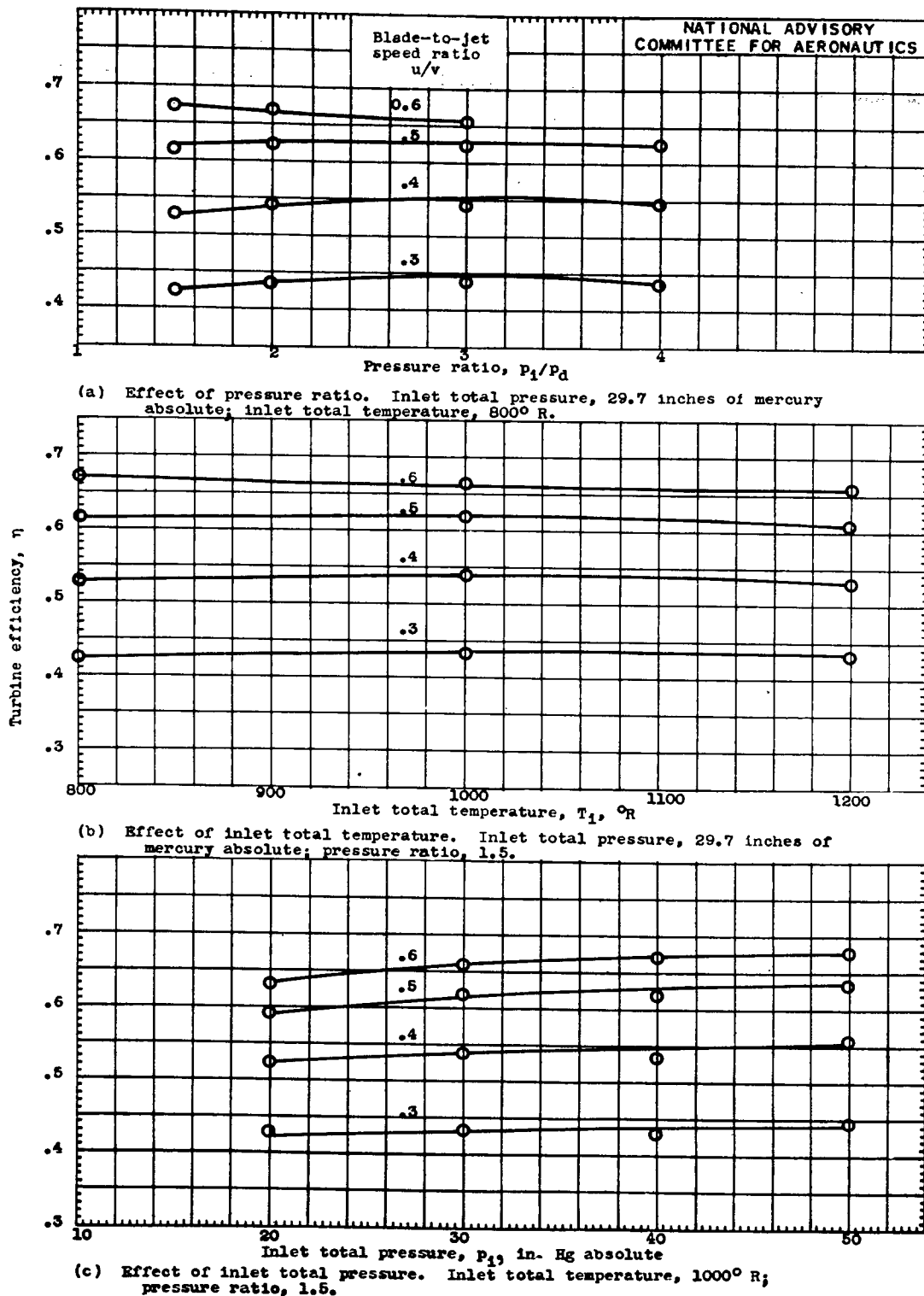
(a) Effect of pressure ratio. Inlet total pressure, 29.7 inches of mercury absolute; inlet total temperature, 800° R.

(b) Effect of inlet total temperature. Inlet total pressure, 29.7 inches of mercury absolute; pressure ratio, 1.5.

(c) Effect of inlet total pressure. Inlet total temperature, 1000° R; pressure ratio, 1.5.

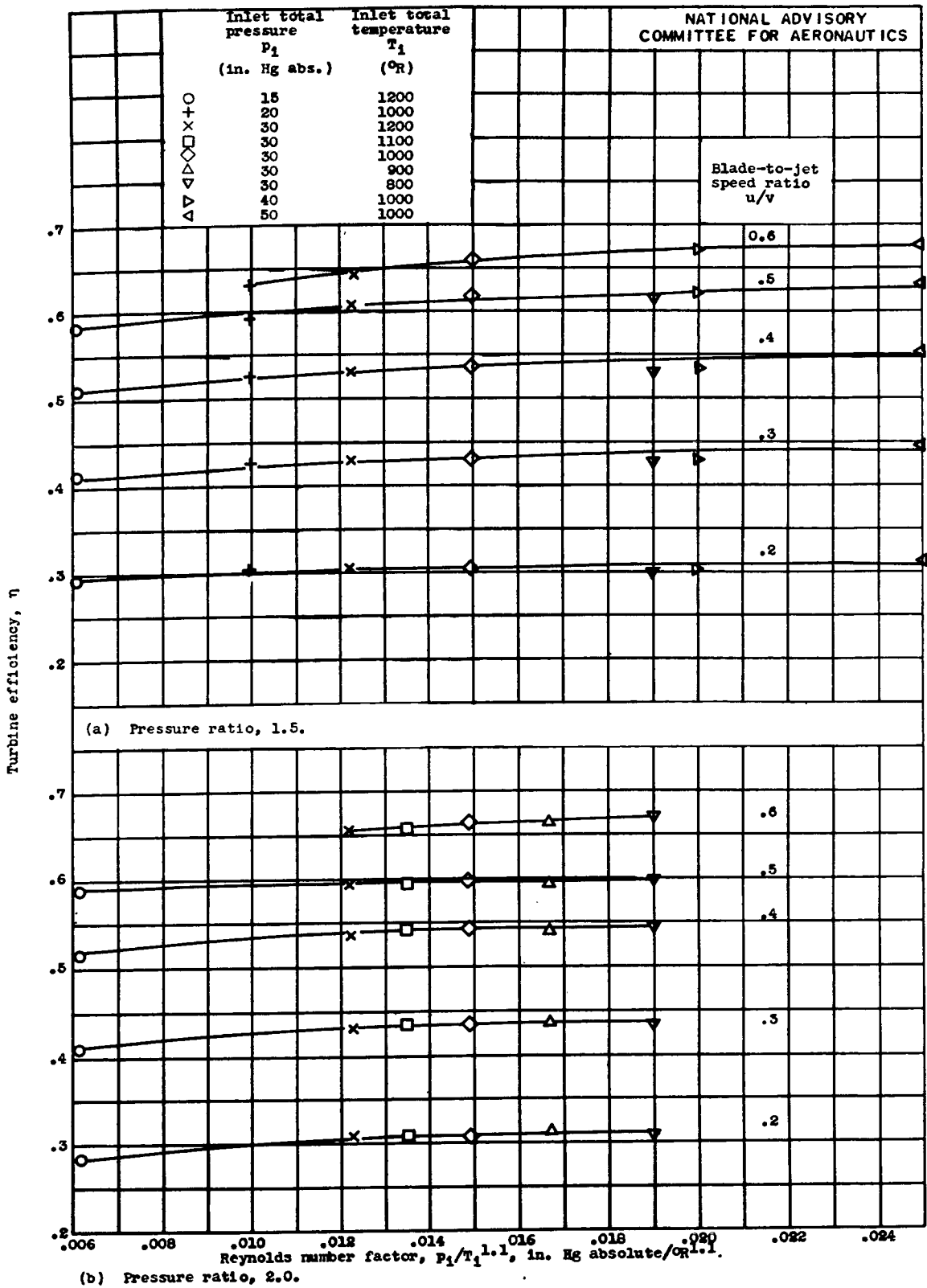Figure 6. — Variation of turbine efficiency with pressure ratio, inlet total temperature, and inlet total pressure.

	Inlet total pressure P_1 (in. Hg abs.)	Inlet total temperature T_1 (°R)
O	15	1200
+	20	1000
×	30	1200
□	30	1100
◇	30	1000
△	30	900
▽	30	800
▷	40	1000
◁	50	1000

NATIONAL ADVISORY
COMMITTEE FOR AERONAUTICS

Blade-to-jet speed ratio u/v

(a) Pressure ratio, 1.5.

(b) Pressure ratio, 2.0.

Reynolds number factor, $P_1/T_1^{1.1}$, in. Hg absolute/°R$^{1.1}$.

Figure 7. — Variation of turbine efficiency with Reynolds number factor.

		Inlet total pressure P_1 (in. Hg abs.)	Inlet total temperature T_1 ($^\circ R$)					NATIONAL ADVISORY COMMITTEE FOR AERONAUTICS
	+	20	1000					
	×	30	1200					
	□	30	1100					
	◇	30	1000					Blade-to-jet speed ratio u/v
	△	30	900					
	▽	30	800					
	▷	40	1000					
	◁	50	1000					

(c) Pressure ratio, 3.0.

Turbine efficiency, η

Reynolds number factor, $p_1/T_1^{1.1}$, in. Hg absolute/$^\circ R^{1.1}$.

(d) Pressure ratio, 4.0.

Figure 7. - Concluded.

The plot shows Gas-flow factor, $M_t \sqrt{\theta}/\delta$, slug/sec (vertical axis) versus Turbine-speed factor, $N/\sqrt{\theta}$, rpm (horizontal axis).

	Inlet total pressure p_1 (in. Hg abs.)	Inlet total temperature T_1 ($^\circ$R)
○	15	1200
+	20	1000
×	30	1200
□	30	1100
◇	30	1000
△	30	900
▽	30	800
▷	40	1000
◁	50	1000

Pressure ratio p_1/p_d

4.0
3.0
2.0
1.5

Figure 8. – Variation of gas flow with turbine-speed factor.
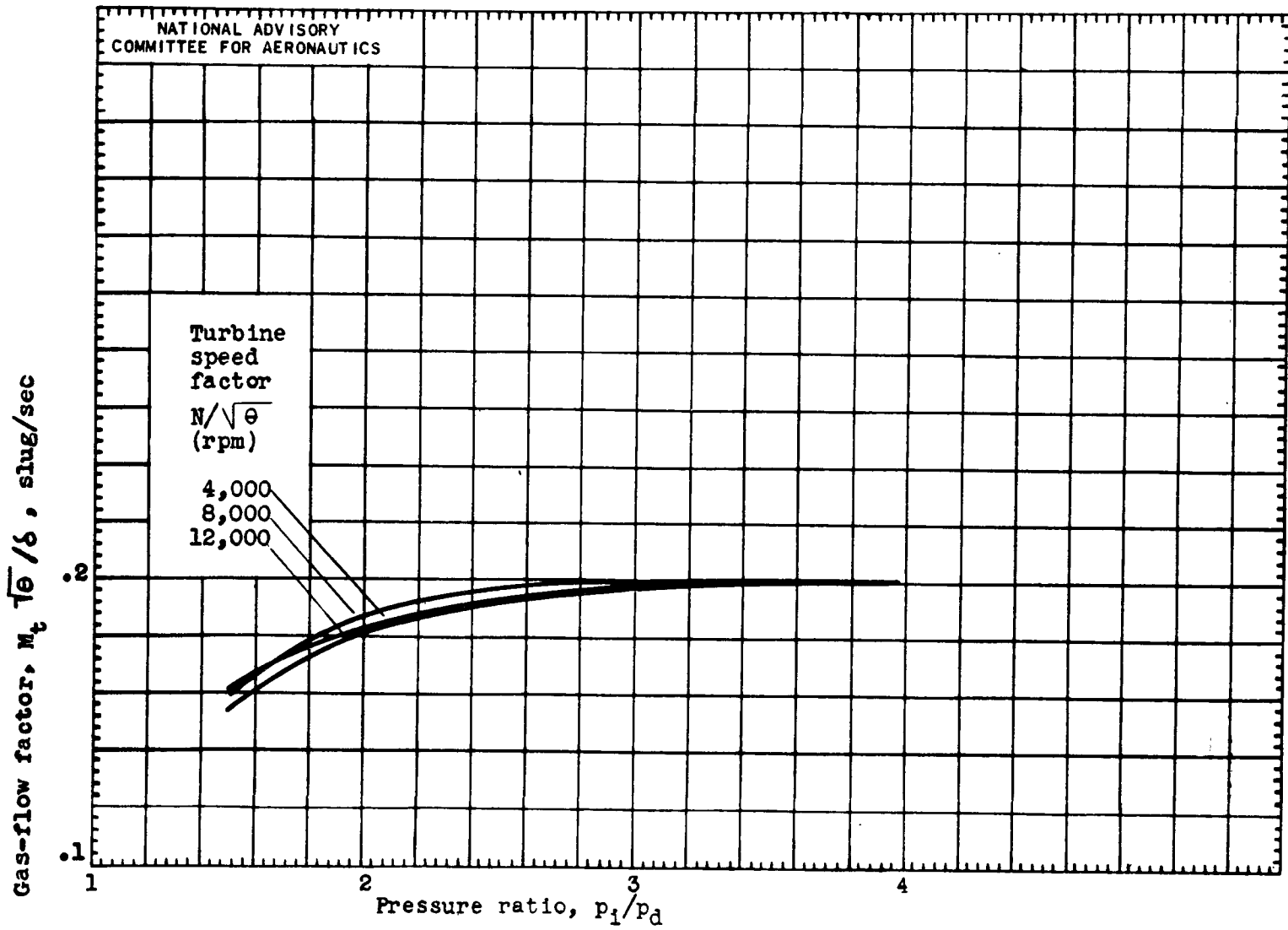
Figure 9. – Variation of gas flow with pressure ratio.

The figure shows a graph with the following labels:

- Title box: NATIONAL ADVISORY COMMITTEE FOR AERONAUTICS
- Y-axis: Gas-flow factor, $M_t \sqrt{\theta}/\delta$, slug/sec
- X-axis: Pressure ratio, p_i/p_d
- Legend: Turbine speed factor $N/\sqrt{\theta}$ (rpm): 4,000; 8,000; 12,000
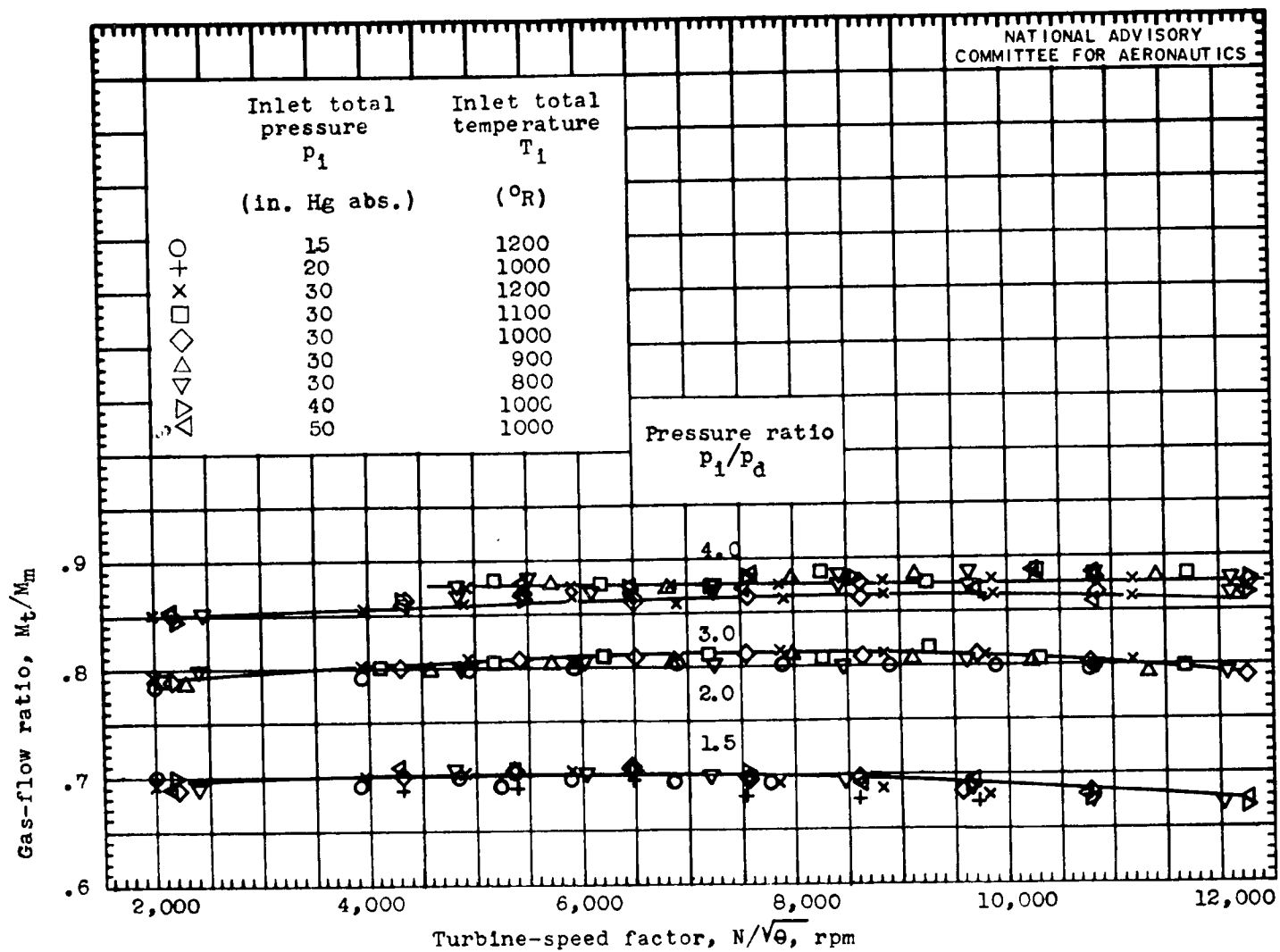
Figure 10. - Variation of the gas-flow ratio M_t/M_m with the turbine-speed factor. $M_m \sqrt{\theta}/\delta$ = 0.228 slug/sec.
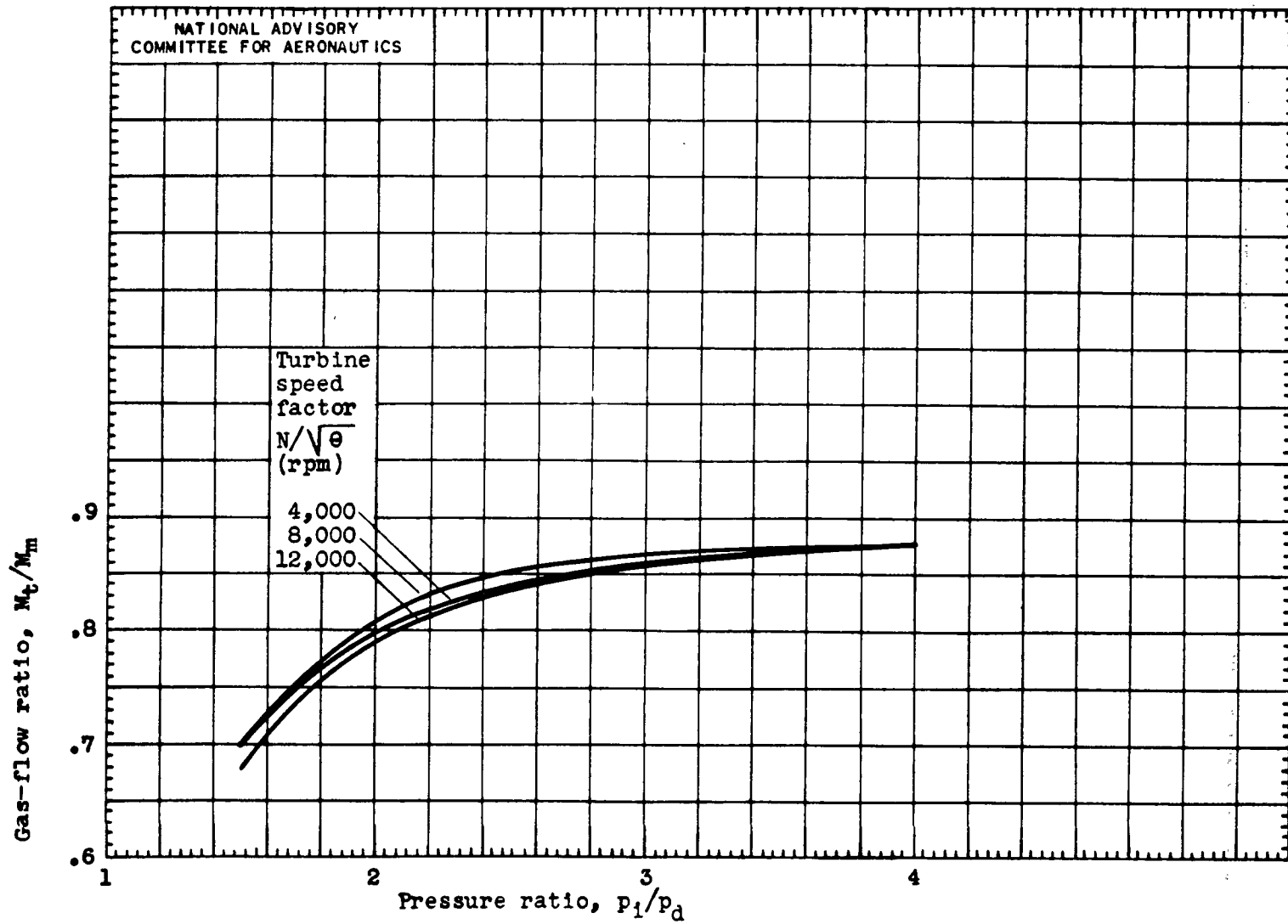
Figure 11. – Variation of gas-flow ratio M_t/M_m with pressure ratio.

(a) Inlet total temperature, 800° R.

(b) Inlet total temperature, 1000° R.

Pressure ratio
P_1/P_d

O	1.5
+	2.0
×	3.0
□	4.0

(c) Inlet total temperature, 1200° R.

Blade-to-jet speed ratio, u/v

Turbine efficiency, η'
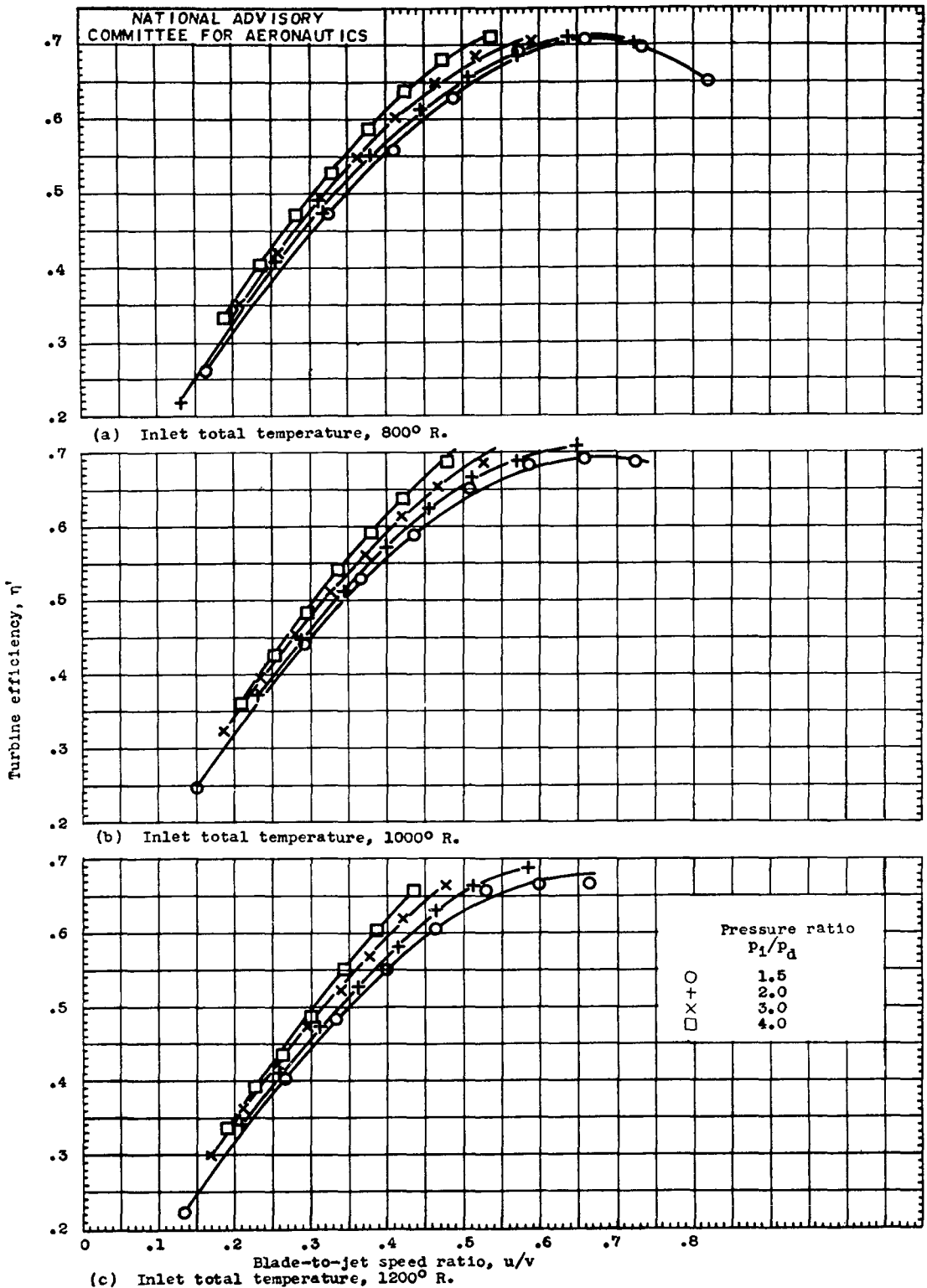
Figure 12. — Variation of the turbine efficiency η' with blade-to-jet speed ratio for various inlet total temperatures and pressure ratios. Inlet total pressure, 29.8 inches of mercury absolute.
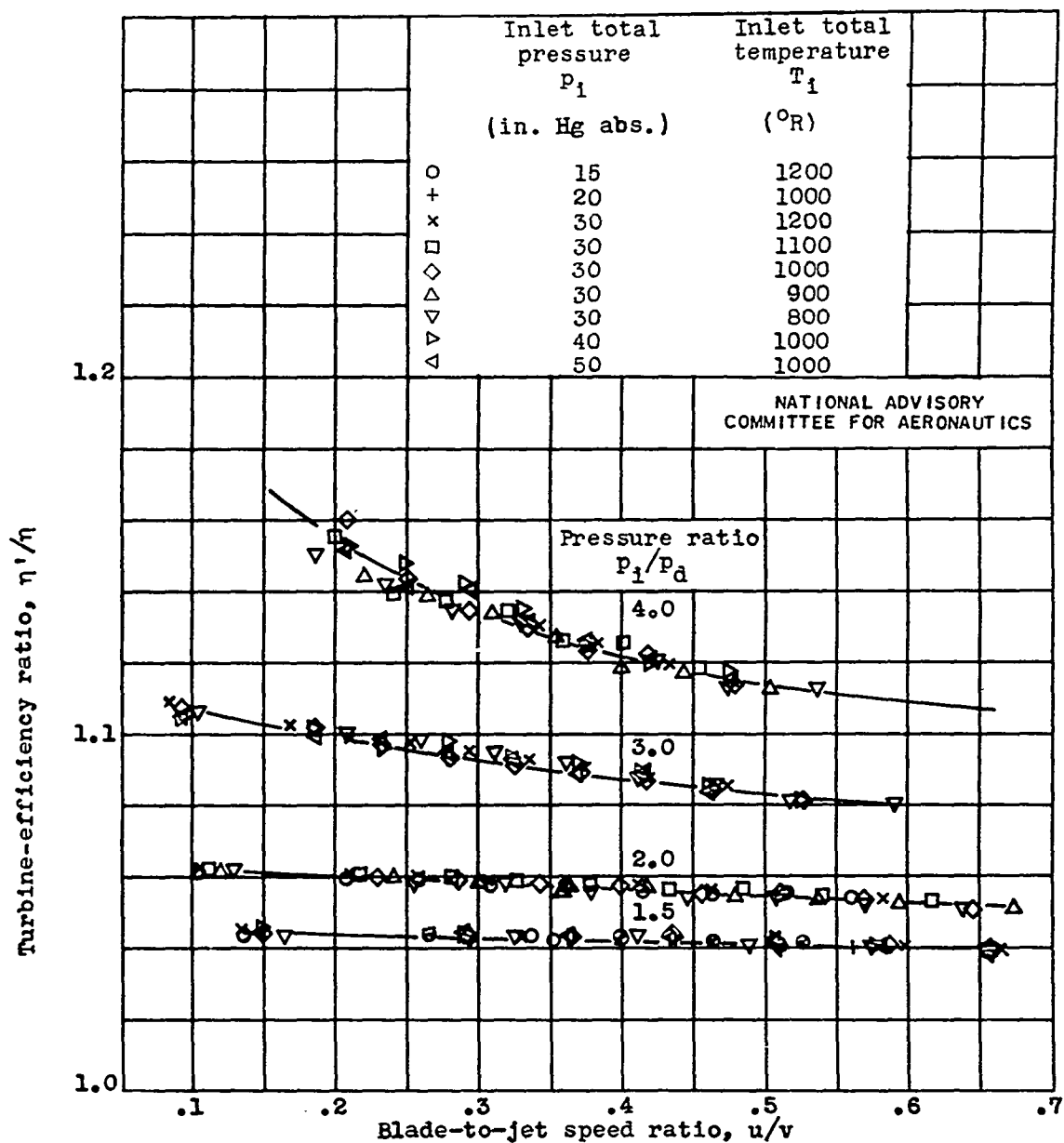
Figure 13. - Variation of turbine-efficiency ratio η'/η with blade-to-jet speed ratio for various pressure ratios.
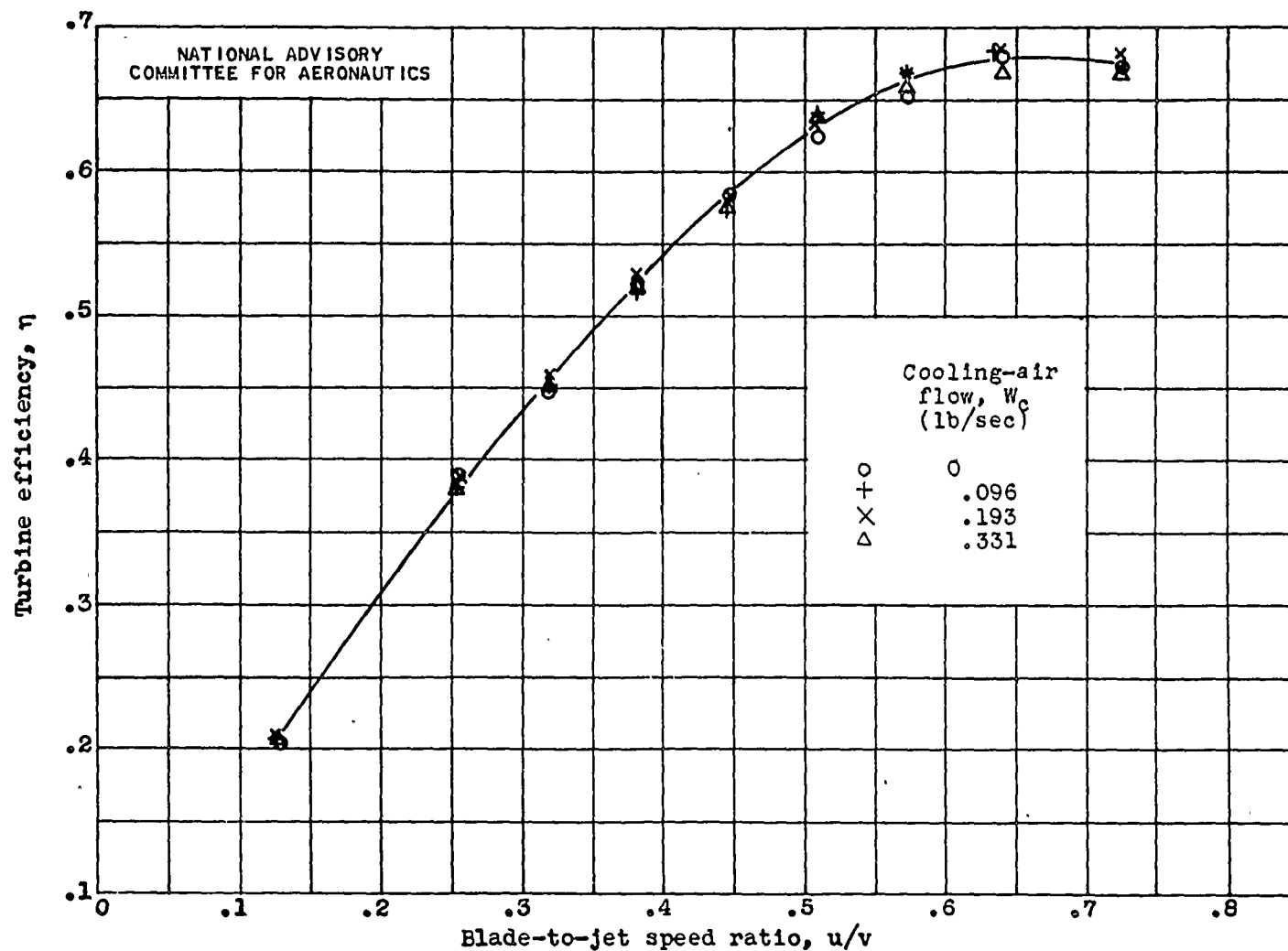
Figure 14. - Variation of turbine efficiency with blade-to-jet speed ratio for various cooling-air flows. Inlet total temperature, 800° R; inlet total pressure, 29.8 inches of mercury absolute; pressure ratio, 2.0.

NATIONAL ADVISORY COMMITTEE FOR AERONAUTICS

WARTIME REPORT

ORIGINALLY ISSUED

July 1946 as
Memorandum Report E6F03

EFFICIENCY OF A RADIAL-FLOW EXHAUST-GAS TURBOSUPERCHARGER

TURBINE WITH A 12.75-INCH TIP DIAMETER

By Earl E. Coulter, Robert G. Larkin, and David S. Gabriel

Aircraft Engine Research Laboratory
Cleveland, Ohio

NACA

WASHINGTON